ResearchGate

See discussions, stats, and author profiles for this publication at: https://www.researchgate.net/publication/258537472

Synthesis and Characterization of Nanoparticles of Calcium Pyrophosphate

Article *in* Modern Physics Letters B · January 2011

DOI: 10.1142/S0217984911025419

CITATIONS
32

READS
142

2 authors:

Sonal Vasant
Saurashtra University
14 PUBLICATIONS **178** CITATIONS
SEE PROFILE

Mihir Janakrai Joshi
Saurashtra University
212 PUBLICATIONS **2,962** CITATIONS
SEE PROFILE

All content following this page was uploaded by Mihir Janakrai Joshi on 02 January 2016.

The user has requested enhancement of the downloaded file.

Modern Physics Letters B, Vol. 25, No. 1 (2011) 53–62
© World Scientific Publishing Company
DOI: 10.1142/S0217984911025419

World Scientific
www.worldscientific.com

SYNTHESIS AND CHARACTERIZATION OF NANOPARTICLES OF CALCIUM PYROPHOSPHATE

SONAL R. VASANT* and M. J. JOSHI†

Department of Physics, Saurashtra University, Rajkot 360 005, India
**sonalvasant@rediffmail.com*
†mshilp24@rediffmail.com

Received 27 October 2009
Revised 22 April 2010

Calcium phosphate based biomaterials play important roles in clinical applications. Calcium pyrophosphate (CPP), a kind of calcium phosphate, can be used as a bone substitution material as well as a bone graft. Because of its similarity to inorganic component of bone and teeth it can be used for surface coating of metallic dental and orthopedic implants. In the present study, calcium pyrophosphate dihydrate (CPPD) nanoparticles were synthesized using surfactant mediated approach. Crystalline nature and average crystallite size was studied using Powder XRD. The CPPD nanocrystallites were found to be triclinic from powder XRD. The TEM study indicated that CPPD nanoparticles were in the range of 13 nm to 20 nm. The presence of various bonds was confirmed by FTIR spectroscopy. The amount of water of hydration and the thermal stability was studied by thermogravimetry. The variations of various dielectric parameters with the frequency of applied field in 3.2 kHz to 32 MHz range and within a temperature range from 60°C to 120°C were studied. The formation of other phases such as β-CPP and α-CPP on heating of CPPD at 900°C and 1250°C, respectively, were studied by the Powder XRD. The results are discussed.

Keywords: Nanoparticles; biomaterials; TEM; TGA; FTIR; powder XRD; dielectric study.

1. Introduction

Calcium phosphate based biomaterials play an important role in clinical applications, especially, as a bone substitution material[1] and as a mild abrasive agent in dentifrices.[2] These materials being biocompatible, provoke little, inflammatory response and connect readily with the bony structure. As a result, they have received considerable attention as bone substitution.[3] The chemical compositions, physical characteristics and crystal structures certainly play important roles in the biological behaviors of calcium phosphate compounds.[4] The biological response of β-calcium pyrophosphate (β-CPP, β-$Ca_2P_2O_7$) for new bone formation is quite similar to that of the hydroxyapatite.[5] Sintered dicalcium pyrophosphate (SDCP), a synthetic compound, has been proven to be more biocompatible to bone tissue than hydroxyapatite.[6] $Ca_2P_2O_7$ with addition of sodium phosphate ceramic is

developed as a bioresorable bone substitute material.[7] Also, other applications of calcium phosphates include repair of periodontal defects, sinus lifts, tooth replacement, spine fusion, ear and eye implants, and delivery systems of drugs.[8] A detailed review on calcium phosphate based osteoinductive materials is written by LeGeros.[9] Altogether, the deposition of CPPD crystals is responsible for the diseases like pseudogout, an acute arthritic attack with pain and inflammation of joints[10,11] and Coffin Lowry Syndrome (CLS), a heritable disorder characterized by pronounced mental retardation and vertebrae abnormalities.[12,13] Brown *et al.*[14] have reported the synthesis of different twenty-five calcium pyrophosphates, among them eight containing ammonium, ten containing potassium and two pairs of dimorphic-hydrated CPP. CPP exists in three polymorphic forms, α-CPP, β-CPP and γ-CPP, each of which is meta-stable at room temperature and formed progressively upon thermal heating of calcium hydrogen phosphate dihydrate (CHPD).[15]

$$\mathrm{CaHPO_4 \cdot 2H_2O} \xrightarrow{135^\circ\mathrm{C}} \mathrm{CaHPO_4} \xrightarrow{360-450^\circ\mathrm{C}} \mathrm{amorphous - Ca_2P_2O_7} \xrightarrow{530^\circ\mathrm{C}}$$
$$\gamma - \mathrm{Ca_2P_2O_7} \xrightarrow{750^\circ\mathrm{C}} \beta - \mathrm{Ca_2P_2O_7} \xrightarrow{1171-1191^\circ\mathrm{C}} \alpha - \mathrm{Ca_2P_2O_7} \xrightarrow{1352^\circ\mathrm{C}} \mathrm{melt}. \quad (1)$$

To the best of the present authors' knowledge, no major work has been reported on the synthesis and characterization of pyrophosphate nanoparticles, except the recent reports of synthesis and characterization of CPPD nanoparticles,[16] manganese pyrophosphate,[17] cobalt-iron pyrophosphate[18] and cerium and titanium pyrophosphates.[19]

The high surface-to-volume ratio present in nanoparticles is expected to alter its properties and applications. In the present investigation, nanocrystalline CPPD has been synthesized by the surfactant mediated approach and characterized by TEM, powder XRD, FTIR, TGA and dielectric studies. The other phases of CPP, such as β-CPP and α-CPP, were obtained on heating the nanoparticles of CPPD at different temperatures and were identified by powder XRD.

2. Experimental Technique

Surfactant mediated approach proposed by Uota *et al.*[20] was used to prepare CPPD nanoparticles. An equal amount of 0.25 M aqueous solution of sodium pyrophosphate ($Na_4P_2O_7$) and 0.5 M aqueous solution of calcium nitrate tetrahydrate ($Ca(NO_3)_2 \cdot 4H_2O$) were prepared. $Na_4P_2O_7$ solution was added in a drop-wise manner into the mixture of $Ca(NO_3)_2 \cdot 4H_2O$ and surfactant with constant stirring at 50°C. The water to surfactant ratio was maintained at 5:1. A non-ionic surfactant Octoxynol-9 was used. The resulting precipitates were quickly filtered, washed with deionized water and air-dried. The AR grade chemicals were used for the synthesis.

In order to obtain different forms of CPP, the synthesized CPPD nanoparticles were heated by placing them in ceramic crucibles in the muffle furnace. The samples were heated at 900°C for one hour and at 1250°C for 15 minutes. At these temperatures, two different forms of CPP are reported as stable.[15] For heating the

samples, Therelek furnace was used with graphite rod at a maximum temperature of 1500°C. The powder XRD was carried out on PHILIPS X'PERT MPD using Cu-K_α radiation. The computer software powder-X was used to analyze the data. The TEM images were recorded on PHILIPS TECNAI using EHT potentials 200 kV. The FTIR spectrum was recorded on Thermo Nicolet 6700 in the range of 400 cm^{-1} to 4000 cm^{-1} using KBr medium. The thermogravimetry was carried out using NETZSCH Geratebau GmbH in the atmosphere of nitrogen in the range of room temperature to 700°C with a heating rate of 15°C/minute. The dielectric study was carried on pelletized samples by using SOLARTRON IMPEDANCE GAIN PHASE ANALYZER SI-1260 in the frequency range from 3.2 kHz to 32 MHz.

3. Results and Discussion

Two common polymorphs of CPPD were identified, which are triclinic CPPD (t-CPPD)[21] and monoclinic CPPD (m-CPPD).[14] Both forms have been observed *in vivo* by Pritzker[22] and the existence of a third hexagonal polymorph was also suggested.[23] The structure of β-calcium pyrophosphate was studied by Webb *et al.*[24] and α-calcium pyrophosphate was studied by Hill.[25]

3.1. *Powder XRD*

Figure 1(a) shows the powder XRD pattern of CPPD nanoparticles. The peak broadening in XRD pattern reflects the nanocrystalline nature of the sample. Scherrer's formula was applied to estimate the average crystallite size as follows:

$$\text{Average crystallite size} = 0.9\lambda/\beta\cos\theta\,, \tag{2}$$

where 0.9 = constant, $\lambda = 1.5418$ Å (wavelength of X-ray radiation), β = full width at half maximum, and θ = diffraction angle.

The average crystallite size for CPPD nanoparticles was found to be 4 nm, whereas, it was found to be 76 nm and 119 nm for the samples heated at 900°C and 1250°C, respectively.

The powder XRD data were analyzed by computer software Powder-X. The triclinic system was found with unit cell parameters, $a = 7.365$ Å, $b = 8.287$ Å, $c = 6.691$ Å, $\alpha = 102.96°$, $\beta = 72.73°$ and $\gamma = 95.01°$, which correspond to that reported in the literature.[21] Therefore, the CPPD nanoparticles are termed as t-CPPD. Figure 1(b) shows the powder XRD pattern of nanocrystalline t-CPPD heated at 900°C for 1 hour. The planes assigned to the reflections closely matched those of reported β-CPP and the tetragonal structure was identified with unit cell parameters, $a = b = 6.684$ Å, $c = 24.145$ Å (JCPDS No. 20-0024).[24] Figure 1(c) shows the powder XRD pattern for the sample heated at 1250°C for 15 minutes. The orthorhombic structure with unit cell parameters, $a = 8.524$ Å, $b = 12.646$ Å, $c = 5.309$ Å was found. The reflections in Fig. 1(c) closely matched with the standard reflections of α-CPP (JCPDS No. 09-0345).[25] It was noted that on heating t-CPPD nanoparticles, the phase transitions into β-CPP and α-CPP occurred

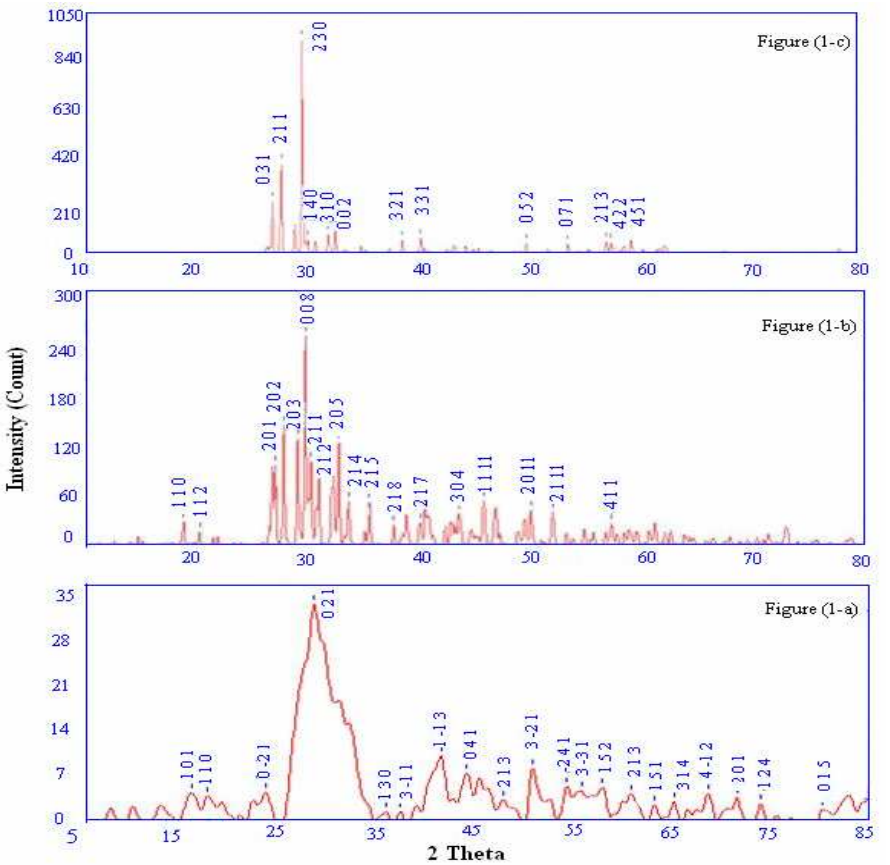

Fig. 1. Powder XRD patterns of pure and heated nanocrystalline CPPD.

and, moreover, the reflections in the powder XRD patterns became more sharp, indicating highly crystalline nature and larger crystallite size.

3.2. *TEM study*

The morphology of t-CPPD nanoparticles as well as the particle size was studied by TEM. Figure 2 shows the TEM image of t-CPPD nanocrystalline particles with different morphologies and the particle size varies between 13 nm to 20 nm as marked on the micrograph.

3.3. *FTIR spectroscopy*

Figure 3 shows the FTIR spectrum of t-CPPD nanocrystalline particles. The broad absorption occurring at 3417.5 cm^{-1} is due to $-OH$ stretching vibration. The

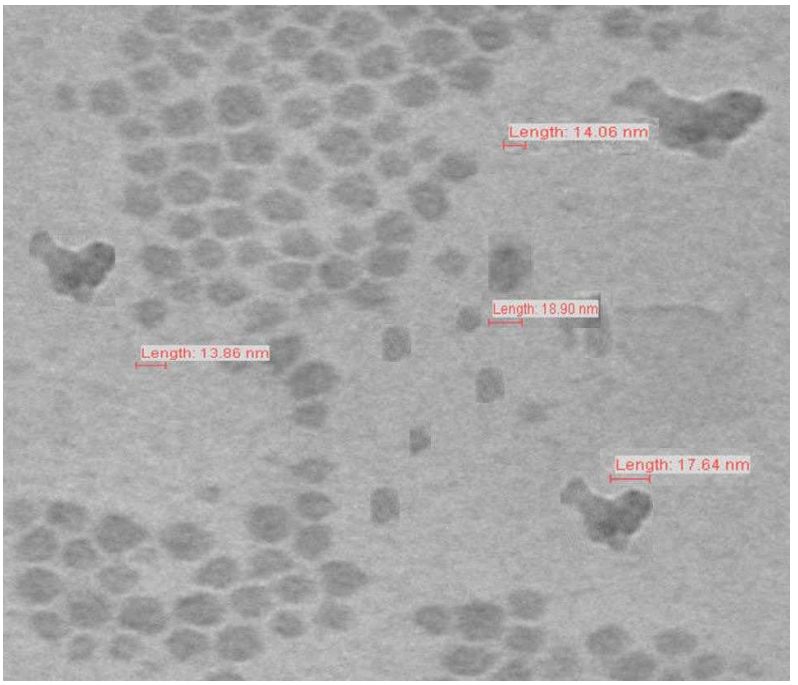

Fig. 2. TEM image of CPPD nanocrystalline particles.

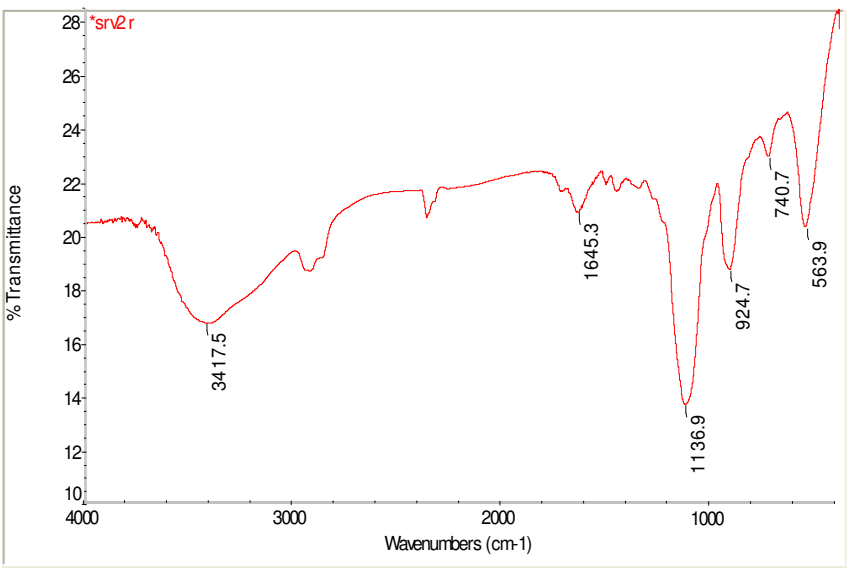

Fig. 3. FTIR spectrum of CPPD nanocrystalline particles.

absorption observed at 1645.3 cm^{-1} is attributed to OH plane bending. As the strength of P–O bond in the P–O–P bridge is weaker than in the $(PO_2)^{2-}$ radical, the stretching frequencies of the P–O–P bridge are expected to be lower than those in the $(PO_2)^{-2}$ radical. The asymmetric and symmetric stretching frequencies of the $(PO_2)^{2-}$ radical are generally observed in the frequency areas 1200–1000 cm^{-1}, 1000–800 cm^{-1}, respectively.[18] In the present investigation, it is observed around 1136.9 cm^{-1} and 924.7 cm^{-1}, respectively. Asymmetric P–O–P bridge vibrations are observed at 740.7 cm^{-1}. Metal–oxygen stretching vibrations are observed at the 563.9 cm^{-1}.

3.4. *TGA study*

Figure 4 shows the thermogram of a t-CPPD nanocrystalline sample. From the thermogram, it can be observed that the sample expels all water molecules slowly on heating around 200°C and becomes anhydrous. The anhydrous sample remains stable up to 700°C, which shows high stability of the compound.[16] From the thermogram, it has been estimated that two water molecules are attached with the nanocrystalline samples, which confirms the dihydrate form of CPP. Table 1 shows theoretically calculated weight percent and experimentally obtained weight percent at different temperatures.

The kinetic and thermodynamic parameters for the dehydration of t-CPPD nanocrystalline samples were evaluated from the thermogram. For the estimation of the kinetic parameters, the Coats and Redfern relation[26] was used, which is discussed in detail elsewhere.[27] Thermodynamic parameters for the dehydration of t-CPPD nanocrystalline sample were calculated using the standard formulae.[28]

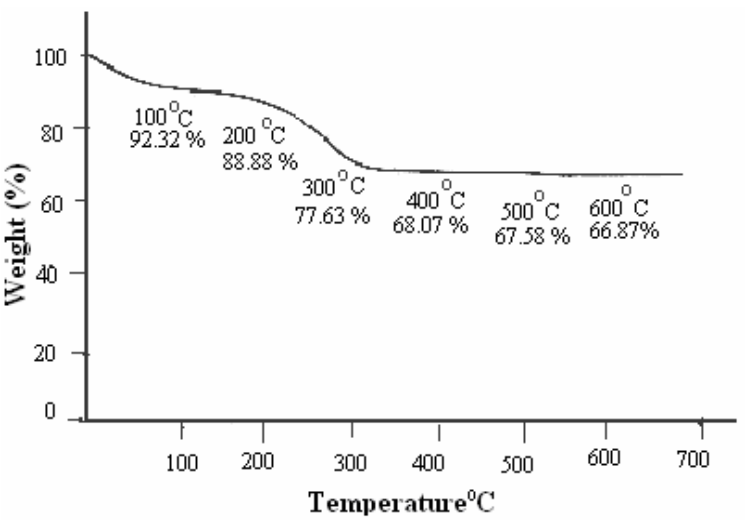

Fig. 4. Thermogram of t-CPPD nanocrystalline particles.

Table 1. Theoretically and experimentally obtained weight percent at different temperatures.

Temperature (°C)	Substance	Theoretically calculated (weight %)	Experimentally observed (weight %)
Room temperature	$Ca_2P_2O_7 \cdot 2H_2O$	100	100
210°C	$Ca_2P_2O_7$	87.58	88

Table 2. Values of thermodynamic and kinetic parameters of CPPD nanoparticles.

Kinetic parameters	Thermodynamic parameters
Activation energy (E) = 10.45 kJ/mole	Standard change in enthalpy ($\Delta^{\#}H^{\circ}$) = 18.53 J/mole
Frequency factor (A) = 1.0646×10^{12}	Standard change in entropy ($\Delta^{\#}S^{\circ}$) = 1.343 kJ/Kmole
Order of reaction (n) = 0	Standard change in Gibbs free energy ($\Delta^{\#}G^{\circ}$) = −8.810 kJ/mole

Table 2 gives the values of different kinetic and thermodynamic parameters. The positive values of standard change in enthalpy ($\Delta^{\#}H^{\circ}$) and standard change in entropy ($\Delta^{\#}S^{\circ}$) and the negative value of standard change in Gibbs free energy ($\Delta^{\#}G^{\circ}$) suggested that the reaction will be spontaneous at higher temperatures.[29]

3.5. *Dielectric study*

Bian[30] have reported the microwave dielectric properties of CPP. Parekh and Joshi[31] have reported dielectric study of the gel-grown m-CPPT (monoclinic calcium pyrophosphate tetra hydrate) crystals. Investigation of dielectric properties is of special interest for some biomaterial applications because it has been reported that electrical field can accelerate the healing of fractures in bones.[32] Also an electrical stimulation enhances the rate of bone growth for bone grafts in spinal fusion.[33] Looking at this, variations in the dielectric constant, the dielectric loss, the AC conductivity and the AC resistivity values with the frequency of applied field in the 3.2 kHz to 32 MHz range is explored. The same experiment was carried out at various temperatures ranging from 60°C to 120°C by heating the samples using small resistive heater attached to the sample holder.

Figure 5(a) shows the variations of dielectric constant with frequency of applied field. It can be noticed from the figure that the dielectric constant decreases as the frequency increases. Initially, the dielectric constant decreases rapidly with increasing frequency and then slowly decreases at higher frequency. This type of behavior indicates higher space charge polarizability of the material in the low frequency region. As the frequency increases, the dipoles cannot comply with the varying external field and, therefore, the polarization decreases and hence the value of dielectric constant decreases as the frequency increases.[34] It is found that as

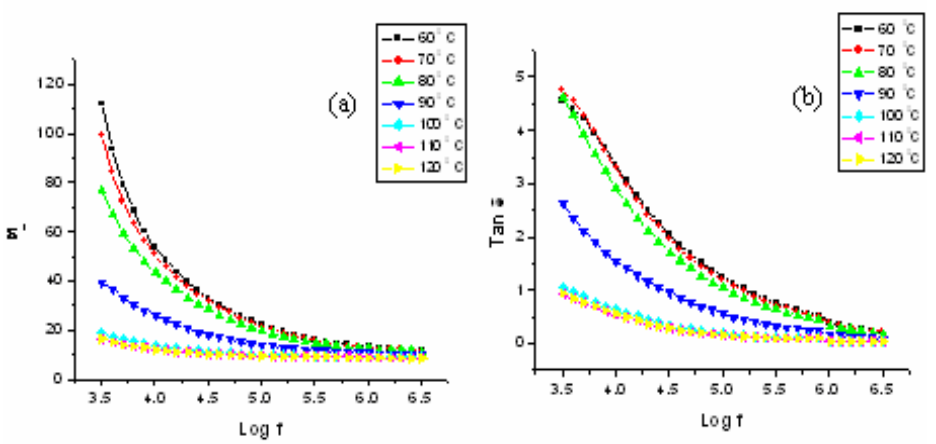

Fig. 5. (a) Variation of dielectric constant and (b) dielectric loss tan δ with frequency of applied field for different temperatures.

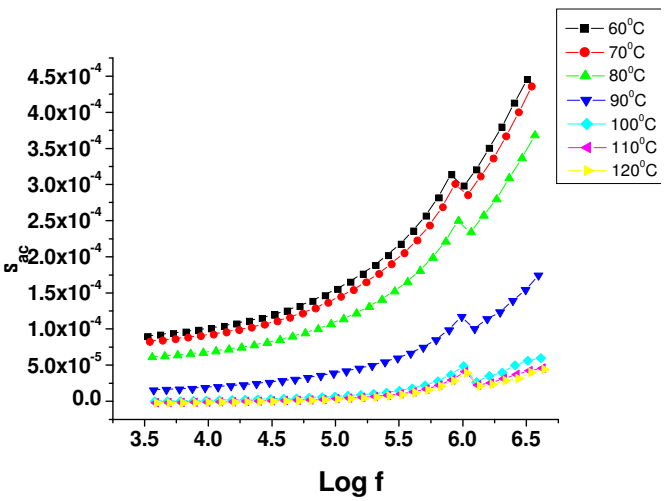

Fig. 6. Variation of AC conductivity with frequency of applied field for different temperatures.

the temperature increases, the dielectric constant decreases which may be due to the dehydration process. There is ion–dipole interaction between dipole moments of water molecules and the effective lattice charges.[35] Thermal energy releases the water molecules from the sample in the dehydration process. The dielectric losses of the samples reflect the chemical and microstructural quality of the samples. Figure 5(b) shows the variation of dielectric loss (tan δ) with frequency of applied field. As the temperature increases, the dielectric loss decreases.

The values of AC resistivity and AC conductivity have been calculated using the standard formulae.[36] Figure 6 shows the frequency dependence of the real part

of AC conductivity at different temperatures. The AC conductivity increases as the frequency of the applied field increases but as the temperature increases, the AC conductivity decreases which may be due to the loss of water.[37] The reverse nature was observed for the AC resistivity.

4. Conclusion

CPPD nanoparticles were synthesized using surfactant mediated approach. The peak broadening in powder-XRD pattern suggested the nanostructured nature with triclinic system and the average particle size was estimated to be 4 nm. From the TEM, it was confirmed that the particle size varied between 13 nm to 20 nm. Heating of t-CPPD nanoparticles at 900°C and 1250°C temperatures in a muffle furnace yielded β-CPP and α-CPP phases of CPP, respectively, which was confirmed by Powder XRD. FTIR study confirmed the presence of pyrophosphate bonds, metal-oxygen bonding and O–H bond in the structure. TGA confirmed the dihydrate form of CPP and also the kinetic and thermodynamic parameters were calculated for dehydration from the thermogram, which suggested the high thermal stability of the sample. The variation of dielectric constant and dielectric loss suggested that both of the quantities decreased as the frequency increased. The AC conductivity increased as the frequency of applied field increased. The temperature had pronounced influence on the dielectric properties because of the dehydration process.

Acknowledgments

The authors are thankful to the Government of Gujarat for giving financial assistance under the sanctioned project on *Nanoscience and Technology and Environmental Physics*, and Prof. K. N. Iyer and H. H. Joshi (Saurashtra University) for their keen interest. The author (S. R. Vasant) acknowledges the sanction of JRF under UGC Meritorious Students Scheme in Special Assistance Programme. Authors are also thankful to Dr. Kanchan, Physics Department, M. S. University of Baroda, for providing dielectric measurement facility.

References

1. D. Knaack, M. E. P. Goad, M. Aiolova, C. Rey, A. Tofighi, P. Chakravarthy and D. D. Lee, *J. Biomed. Mater. Res. Part B: Appl. Phys.* **43** (1999) 399.
2. M. Cordon and J. Norfleet, United States Patent 3989814 (1976).
3. M. Jarcho, *Clin. Orthop. Rel. Res.* **157** (1981) 259.
4. S. R. Radin and P. Ducheyne, *J. Biomed. Mater. Res.* **28** (1994) 1303.
5. T. Kitsugi, T. Yamamuro, T. Nakamura, S. Kotani and T. Kokubo, *Biomaterials* **4** (1993) 216.
6. J. S. Sun, Y. H. Tsuang, C. J. Liao, H. C. Liu, Y. S. Hang and F. H. Lin, *J. Biomed. Mater. Res.* **37** (1997) 324.
7. F. H. Lin, C. J. Liau, K. S. Chen and C. Y. Wang, *J. Biomed. Eng. Applic. Bas. Commun.* **7** (1995) 515.

8. W. Paul and C. P. Sharma, *Trends Biomater. Artif. Organs* **19** (2005) 7.
9. R. Z. LeGeros, *Chem. Rev.* **108** (2008) 4742.
10. L. M. Ryan and D. J. McCarthy, *Arthritis and Allied Conditions*, ed. W. J. Koopman (Williams and Wikkins, Baltimore, 1997).
11. D. J. McCarthy, *Arthritis and Allied Conditions*, ed. W. J. Koopman (Williams and Wikkins, Baltimore, 1997).
12. G. Blackmore, B. Morton and Z. G. Huang, *Mar. Pollut. Bull.* **36** (1998) 32.
13. W. Fialkowski and W. A. Newman, *Mar. Pollut. Bull.* **36** (1998) 138.
14. E. H. Brown, J. R. Lehr, J. P. Smith and A. W. Faizer, *Agri. Food Chem.* **11** (1963) 214.
15. K. Othmer, *Encyclopedia of Chemical Technology*, Vol. 17 (Interscience, Division of John Wiley & Sons Inc., 1970).
16. S. R. Vasant, K. P. Tank, P. M. Vyas, K. B. Mehta, B. B. Parekh and M. J. Joshi, in *Proc. Int. Conf. Biomed. Engrg. Nano-Technol.*, ed. S. H. Pawar (D. Y. Patil University, Kolhapur, 21–23 October, 2008), p. 166.
17. B. Boonchom and R. Baitahe, *Mater. Lett.* **63** (2009) 2218.
18. B. Boonchom and N. Phuvongpha, *Mater. Lett.* **63** (2009) 1709.
19. W.-W. Wu, Y.-J. Fan, X.-H. Wu, S. Liao, X.-F. Huang and X.-H. Li, *Rare Metals* **28** (2009) 33.
20. M. Uota, H. Arakawa, N. Kitamura, T. Yoshimura, J. Tanaka and T. Kijima, *Langmuir* **21** (2005) 4724.
21. N. S. Mandel, *Acta Crystallogr. Sec. B* **31** (1975) 1730.
22. K. P. H. Pritzker, *Calcium Phosphates in Biological and Industrial Systems*, ed. Z. Amzad (Kluwer, Boston, 1998).
23. G. S. Mandel, K. M. Renne, A. M. Kolbach, W. D. Kalpan, J. D. Miller and N. S. Mandel, *J. Cryst. Growth* **87** (1988) 453.
24. N. C. Webb, *Acta Crystallogr.* **21** (1966) 942.
25. W. L. Hill, G. T. Faust and D. S. Reynolds, *Am. J. Sci.* **242** (1944) 457.
26. A. W. Coats and J. P. Redfern, *Nature* **68** (1964) 201.
27. V. S. Joshi and M. J. Joshi, *Cryst. Res. Technol.* **38** (2003) 817.
28. K. J. Laidler, *Chemical Kinetics* (Harper and Row, New York, 1987).
29. A. G. Whittaker, A. R. Mount and M. R. Hill, *Physical Chemistry* (Viva, New Delhi, 2001).
30. J. Bian, D. Kim and K. S. Hong, *J. Eur. Ceram. Soc.* **23** (2003) 2589.
31. B. B. Parekh and M. J. Joshi, *Cryst. Res. Technol.* **42** (2007) 127.
32. J. T. Ryaby, *Clin. Orthop.* **355** (1998) 205.
33. M. Oishi and S. T. Onesti, *Neurosurgery* **47** (2000) 1041.
34. F. M. Reicha, M. El-Hi-Ti, A. Z. El-Sonabati and A. M. Diab, *J. Phys. D* **24** (1991) 369.
35. K. S. Udupa, P. M. Rao, S. Aithal, A. P. Bhat and D. K. Avasthi, *Bull. Mater. Sci.* **20** (1997) 1069.
36. A. V. Ravi Kumar, B. Apparao and N. Veeraiah, *Bull. Mater. Sci.* **212** (1998) 341.
37. J. P. Gittings, C. R. Bowen, I. G. Turner, F. Baxter and J. Chaudhuri, *J. Eur. Ceram. Soc.* **27** (2007) 4187.